ELSEVIER

Journal of Non-Crystalline Solids 201 (1996) 37–46

JOURNAL OF NON-CRYSTALLINE SOLIDS

Blue and green upconversion fluorescences of Ho^{3+} in fluoride glasses

Xuelu Zou *, Hisayoshi Toratani

R&D center, Hoya Corporation, 3-3-1 Musashino Akishima-shi, Tokyo 196, Japan

Received 24 July 1995; revised 28 November 1995

Abstract

Blue and green upconversion fluorescences at about 424, 485, and 545 nm were observed in Ho^{3+} singly doped fluoride glasses under 647 nm excitation. The relative intensities of these fluorescences for ZrF_4 (HfF_4) based glasses were found to be larger than those for AlF_3 based glasses due to their lower phonon energies. The upconversion efficiency and the emission efficiency of Ho^{3+} doped fluoride systems are primarily dominated by the populations of the corresponding intermediate levels from which a part of the excited ions can be re-excited to the upper emitting levels. Rate equation modeling of the upconversion fluorescence has been established and utilized to reveal the upconversion mechanisms for the Ho^{3+} doped systems. Using this model, the concentration and the excitation dependences of these upconversion fluorescences are well interpreted.

1. Introduction

Upconversion lasers are able to provide a useful route to the development of visible lasers pumped by cheap semiconductor lasers operating in the near infrared region. Some rare earth ions such as Er^{3+}, Ho^{3+} and Tm^{3+}, when incorporated as impurities in sufficient concentration into a suitable host lattice, can upconvert infrared radiation to various shorter wavelengths. Several comprehensive review papers provide details on the upconversion process [1–3]. The practical interest in frequency upconversion arises from the possibility of making infrared beams visible, the opportunity to change infrared light to a spectral region in which efficient detection by photomultipliers or photodiodes can be realized, and the promise of using upconversion pumping for laser device systems. Upconversion lasers using the rare earth ions in crystals and fluoride glasses have been demonstrated in bulk materials and fibers [4–9]. Recently, Allain et al. [10] demonstrated cw upconversion lasing action in Ho^{3+} doped fluorozirconate glass fiber at room temperature. The interesting feature of their work is the linear dependence on pump power despite the fact that the upconversion process requires two or more photons as proposed by them. This feature has been also reported for other upconversion lasers, [6,11] and has not yet received a conclusive explanation. The purpose of this work is to study the excitation and concentration dependences of the upconversion fluorescences corresponding to the $^5G_5$–$^5I_8$, $^5F_3$–$^5I_8$, and $^5S_2$–$^5I_8$ tran-

* Corresponding author. Tel: +81-425 46 2748; fax: +81-425 46 2742; e-mail: hoyafcg1@po.iijnet.or.jp.

PII S0022-3093(96)00130-5

sitions of Ho^{3+} in several fluoride glasses using the rate equation model, and thereby identifying the underlying physical phenomena which give rise to the observed linear dependences on pump power.

2. Experimental procedure

Glass hosts used in this study were prepared by highly purified fluorides as starting materials. The batches were melted in carbon crucibles at 850 to 950°C for 1 to 2 h in argon gas atmosphere. The melts were rapidly cooled to the glass transition temperatures and then annealed. The glass compositions are listed in Table 1. All samples for the optical property measurements were cut and polished by the same process to the size of $25 \times 25 \times 5$ mm^3.

Fluorescence spectra were measured by exciting the samples with a krypton laser operating at 647 nm. The pumping light was chopped at 80 Hz and focused on the 25×25 mm^2 face of sample. The position of 1 mm from an edge of sample was excited to minimize the re-absorption of emission. Average beam size of pumping light through sample was about 0.5 mm^2. The fluorescence from the 25×5 mm^2 face was focused onto a monochromater and detected by a R-2228 photomultiplier tube. The signal was intensified with a lock-in amplifier and processed by a computer. The errors in these measurements were estimated to be $< \pm 5\%$. Fluorescence lifetimes were measured by exciting the samples with a Nd:YAG laser pumped Rhotamine-101 dye laser operating around 645 nm, and the fluorescences were detected with the R-2228 photomultiplier tube and a InAs detector. The fluorescence decay curves were recorded and averaged with a computer controlled transient digitizer. The errors in the lifetime measurements were estimated to be $< \pm 10\%$.

3. Experimental results

Initial spectroscopic studies were carried out using krypton laser operating at 647 nm which corresponds to the $^5I_8$–$^5F_5$ absorption as a pump source. Upconversion fluorescences corresponding to the $^5G_5$–$^5I_8$, $^5F_3$–$^5I_8$, and $^5S_2$–$^5I_8$ transitions were observed at about 424, 485, and 545 nm in various fluoride glasses, respectively. Fig. 1 shows, for example, the fluorescence spectrum of 0.5 mol% Ho^{3+} doped AZF glass. The fluorescence intensities, evaluated from the fluorescence bands in Fig. 1, decrease in the order of $^5S_2$–$^5I_8 > {}^5F_3$–$^5I_8 > {}^5G_5$–$^5I_8$ due to the differences in their upconversion efficiencies and their energy gaps to the nearest lower levels. The latter effect seems to be especially important, since the fluorescence intensity increases in the order of increasing the energy gaps with a linear relationship as shown in Fig. 2.

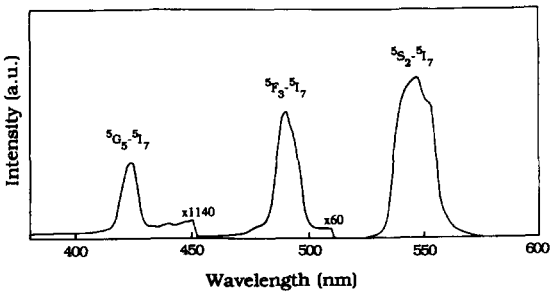

Fig. 1. Emission spectrum of 0.5 mol% Ho^{3+} doped AZF glass excited by a krypton laser at 647 nm. Dashed lines indicate scale changes of factors of 1140 and 60.

Fig. 3 exhibits composition dependences of the $^5G_5$–$^5I_8$, $^5F_3$–$^5I_8$, and $^5S_2$–$^5I_8$ fluorescence intensities for 0.5 mol% Ho^{3+} doped fluoride glasses. The upconversion fluorescences for the Ho^{3+} doped ZrF_4 (HfF_4) based glasses are more intense than those for the Ho^{3+} doped AlF_3 based glasses. This behavior is attributed to lower phonon energies of the ZrF_4 (HfF_4)based glasses of 500–550 cm^{-1} than the AlF_3 based glasses of 600–640 cm^{-1} which were determined via Raman spectroscopy. Generally, the populations of the excited states involving the emitting levels and the intermediate levels from which a part of the excited ions can be re-excited to the upper emitting levels by pump excited state absorption (ESA) are substantially impacted by the non-radiative decay rate that increases as the lattice phonon energy [12] becomes higher. Therefore, the lattice phonon energy of host glass not only affects quantum efficiencies of the emitting levels such as $^5G_5$, $^5F_3$ and $^5S_2$, but also impacts the upconversion efficiencies which are primarily determined by the populations of intermediate levels such as $^5I_6$ and

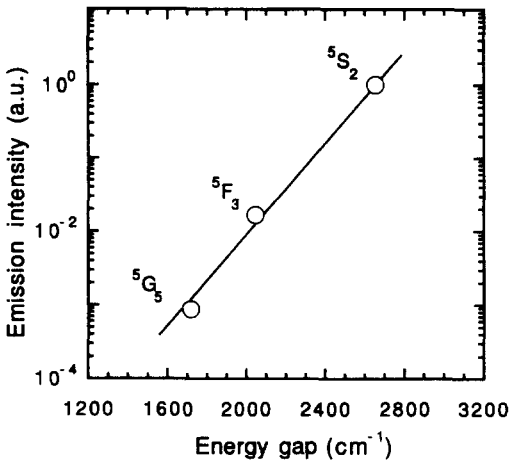

Fig. 2. Relative intensities of upconversion fluorescences originating from the $^5G_5$, $^5F_3$, and $^5S_2$ levels of Ho^{3+} versus the energy gaps from these levels to the nearest lower levels. Line is a guide to the eye.

$^5I_7$. Clearly, the excitation populations of intermediate levels and the quantum efficiencies of emitting levels of Ho^{3+} in a host glass with a lower phonon energy are undoubtedly higher than those in a glass with a higher phonon energy. Consequently, for enhancing the upconversion efficiency and fluorescence of Ho^{3+} doped system, the glass with lower lattice phonon energy is available as the host medium.

The relative intensities of the $^5G_5$–$^5I_8$, $^5F_3$–$^5I_8$, and $^5S_2$–$^5I_8$ upconversion fluorescences are plotted in Fig. 4 as a function of the Ho^{3+} concentration in AZF glass. The pump power for the upconversion excitation was about 80 mW. It is apparent from Fig. 4 that when the Ho^{3+} concentration is increased, the $^5F_3$–$^5I_8$ fluorescence intensity increases monotonically, while the $^5G_5$–$^5I_8$ and $^5S_2$–$^5I_8$ fluorescence intensities increase initially and decrease after the maximum values occurred. The concentration depen-

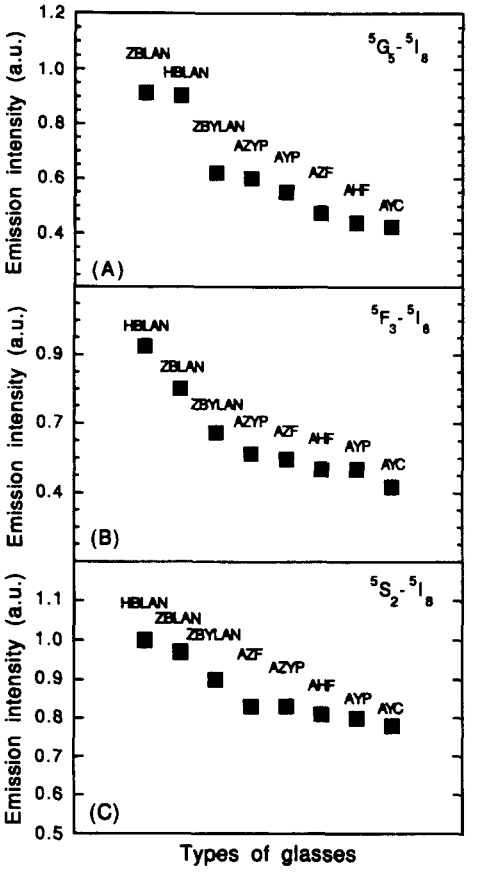

Fig. 3. Relative intensities of upconversion fluorescences originating from the $^5G_5$, $^5F_3$, and $^5S_2$ levels of Ho^{3+} in various fluoride glasses excited at 647 nm.

Table 1
Composition of fluoride glasses used in this study (mol%)

Glass	ZrF_4	HfF_4	AlF_3	YF_3	LaF_3	MgF_2	CaF_2	SrF_2	BaF_2	PbF_2	NaF	HoF_3
ZBLAN	53.00	–	3.00	–	3.50	–	–	–	20.00	–	20.00	0.50
HBLAN	–	53.00	3.00	–	3.50	–	–	–	20.00	–	20.00	0.50
ZBYLAN	32.59	11.87	8.09	5.58	3.03	–	–	–	26.58	9.80	1.96	0.50
AZF	13.00	–	25.00	$11 - X$ [a]	–	4.00	15.00	13.70	12.70	–	5.60	X
AHF	–	12.00	27.00	8.50	–	3.50	18.30	13.60	12.60	–	4.00	0.50
AZYP	10.00	–	27.00	12.50	–	4.00	16.00	–	10.00	20.00	–	0.50
ZYP	–	–	35.00	14.50	–	5.00	15.00	–	10.00	20.00	–	0.50
AYC	–	–	34.50	13.00	–	8.90	26.00	8.90	8.20	–	–	0.50

[a] $X = 0.1$, 0.2, 0.5, 1.0, 2.0, 4.0, and 8.0 mol% HoF_3.

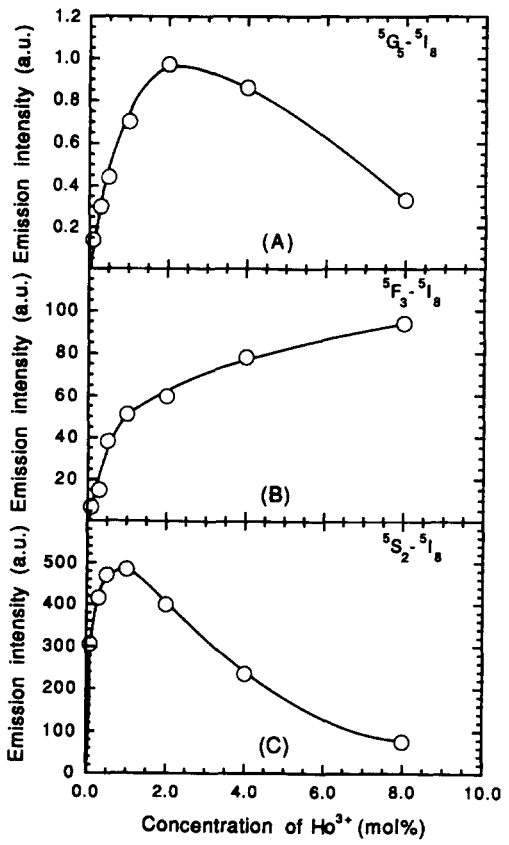

Fig. 4. Concentrational dependences of upconversion fluorescence intensities corresponding to the $^5G_5$–$^5I_8$, $^5F_3$–$^5I_8$, and $^5S_2$–$^5I_8$ transitions of Ho^{3+} in AZF glass excited at 647 nm. Lines are a guide to the eye.

dence of the $^5F_3$–$^5I_8$ fluorescence is distinguishable from those of the $^5G_5$–$^5I_8$ and $^5S_2$–$^5I_8$ fluorescences. It indicates that the upconversion processes for populating these upper emitting levels may be different.

In order to understand differences in the concentration dependences of these upconversion fluorescences, the $^5G_5$, $^5F_3$, and $^5S_2$ lifetimes were measured for Ho^{3+} doped AZF glass. In these measurements, the emission levels were excited by absorbing second photon from the corresponding intermediate levels such as $^5I_6$ and $^5I_7$. The decay times for the $^5G_5$–$^5I_8$ and $^5F_3$–$^5I_7$ transitions were found to be nearly exponential and their lifetimes evaluated from the e-folding time values do not vary with the Ho^{3+} concentration as shown in Fig. 5. However, the

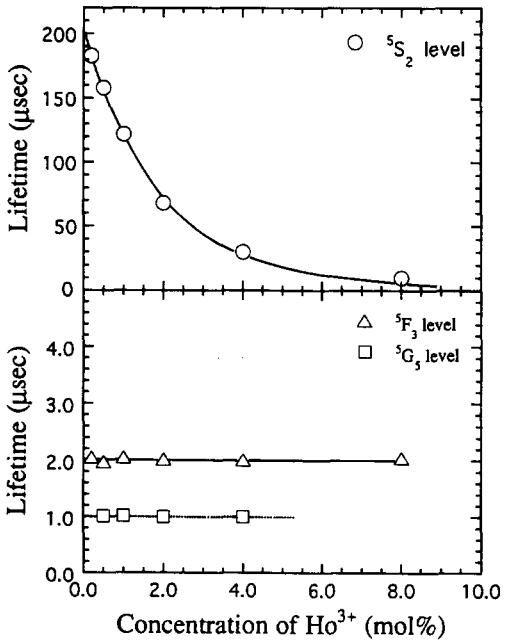

Fig. 5. Concentrational dependences of the $^5G_5$, $^5F_3$, and $^5S_2$ lifetimes of Ho^{3+} in AZF glass excited at 645 nm. Lines are a guide to the eye.

$^5S_2$–$^5I_8$ fluorescence decays non-exponentially and its lifetime decreases strongly as the Ho^{3+} concentration increases. These results indicate that the en-

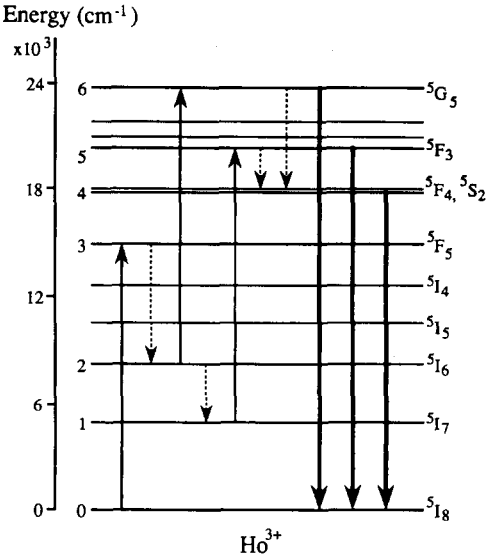

Fig. 6. Upconversion excitation mechanisms for Ho^{3+} doped fluoride glass. Energy levels are used in theoretical rate equation model.

ergy transfers from the $^5G_5$ and $^5F_3$ levels are possibly inexistent, while the efficient energy transfer for quenching population of the $^5S_2$ level are virtually existent in the system. Obviously, only using the above lifetime measurements, the behavior of concentration dependences of the upconversion fluorescences can hardly receive a conclusive explanation. For clarifying this behavior, therefore, the upconversion mechanism and concentration dependences of the populations of intermediate levels for the Ho^{3+} doped system under the 647 nm excitation need further research.

4. Discussion

4.1. Upconversion excitation mechanism for Ho^{3+} doped fluoride glass

The upconversion excitation pathways which was proposed by Allain et al. [10] are shown in Fig. 6. The $^5F_5$ level is fed from the ground state level by ground state absorption. It then depopulates rapidly via non-radiative de-excitation down to the nearest lower metastable $^5I_6$ level. The ions in this level can either de-excite radiatively towards the $^5I_7$ and $^5I_8$ levels, or be brought by ESA to the $^5G_5$ level, from which a part of the excited ions emits towards the ground state and another part feeds into the $^5S_2$ level through the $^5F_3$ level via non-radiative de-excitation. In this case, the $^5F_4$ and $^5S_2$ levels are thermally coupled and can be considered as a whole. Another similar pathway is also shown in Fig. 6, starting from the $^5I_7$ level which is mainly fed from the $^5I_6$ level, i.e., the ions in the $^5I_7$ level can either de-excite radiatively towards the ground state, or be re-excited to the $^5F_3$ level by ESA, from which a part of the excited ions emits and another part feeds into the $^5S_2$ upper level. This excitation mechanism has been proved by the measured fluorescence spectrum for the Ho^{3+} doped AZF glass as shown in Fig. 1. In this spectrum the upconversion fluorescence bands corresponding to the $^5G_5$–$^5I_8$ and $^5F_3$–$^5I_8$ transitions are clearly observed. It indicates that the excitation populations of the emitting levels of $^5G_5$ and $^5F_3$ are built up from the intermediate levels of $^5I_6$ and $^5I_7$ by ESA, respectively. Here it is noteworthy that the non-radiative decay from the $^5F_5$ level to the $^5I_6$ level occurs via a cascade through the $^5I_4$ and $^5I_5$ levels, which are not included in the proposed mechanistic scheme in Fig. 6. The energy gaps between these levels are around 2000 cm^{-1}, which is of the order of about three lattice phonons of the glass hosts. For such a small energy gaps the empirical multiphonon expression fails and the non-radiative decay rate will be much higher than predicted.

To understand theoretically two upconversion excitation pathways as described above, it is interesting to apply rate equations to this system. The rate equation model we will use here is identical to the upconversion mechanism shown in Fig. 6 for the blue fluorescences originating from the $^5G_5$ and $^5F_3$ levels and the green fluorescence from the $^5S_2$ level of Ho^{3+} under 647 nm excitation. The rate equations required to describe this model are

$$\frac{dn_1}{dt} = W_{21}n_2 - \phi U_{15}n_1 - \left(C_1 + \tau_1^{-1}\right)n_1, \tag{1}$$

$$\frac{dn_2}{dt} = W_{32}n_3 - \phi U_{26}n_2 - \left(C_2 + \tau_2^{-1}\right)n_2, \tag{2}$$

$$\frac{dn_3}{dt} = \phi U_{03}n_0 + W_{43}n_4 - \left(C_3 + \tau_3^{-1}\right)n_3, \tag{3}$$

$$\frac{dn_4}{dt} = W_{54}n_5 + W_{64}n_6 - \left(C_4 + \tau_4^{-1}\right)n_4, \tag{4}$$

$$\frac{dn_5}{dt} = \phi U_{15}n_1 - \tau_5^{-1}n_5, \tag{5}$$

$$\frac{dn_6}{dt} = \phi U_{26}n_2 - \tau_6^{-1}n_6, \tag{6}$$

where n_0 and n_i represent the populations of ground state and excited level i, respectively. Transitions between levels i and j of a single ion are denoted by W_{ij} and the lifetime of level i of single ion in the absence of ion–ion transfer is denoted by τ_i (it is inversely proportional to the total of the non-radiative and radiative emission rates). The energy transfer rates comprising so-called concentration quenching rates are denoted by C_i. The absorption cross section for each transitions is U_{ij} and the incident pumping flux is ϕ.

If the steady state fluorescence intensities from levels 4, 5, and 6 are sought, the time derivatives of the level populations are set equal to zero and the

equations can be solved for the excitation populations of the $^5G_5$, $^5F_3$, and $^5S_2$ levels, i.e.,

$$n_6 = \frac{\phi^2 U_{03} U_{26} W_{32} n_0}{\tau_6^{-1}(C_3 + \tau_3^{-1})(C_2 + \tau_2^{-1})}, \quad (7)$$

$$n_5 = \frac{\phi^2 U_{03} U_{15} W_{32} W_{21} n_0}{\tau_5^{-1}(C_3 + \tau_3^{-1})(C_2 + \tau_2^{-1})(C_1 + \tau_1^{-1})}, \quad (8)$$

$$n_4 = \frac{\phi^2 U_{03} W_{32} n_0}{(C_4 + \tau_4^{-1})(C_3 + \tau_3^{-1})(C_2 + \tau_2^{-1})} \times \left[\frac{W_{54} W_{21} U_{15}}{\tau_5^{-1}(C_1 + \tau_1^{-1})} + \frac{W_{64} U_{26}}{\tau_6^{-1}}\right]. \quad (9)$$

In solving these expressions, we have assumed that depopulation rate of a intermediate level by upconversion can be neglected with respect to the spontaneous and non-radiative emission from this level. This approximation that enables the analytic solutions to be simplified is valid, since no significant depopulation of the intermediate levels were observed in this system for the given pump powers.

If we assume that the excitation intensity is sufficiently weak that the ground state is not considerably depopulated, the ground state population of n_0 can be approximated by the total concentration of Ho^{3+} ions, N_0. Then the $^5G_5$–$^5I_8$, $^5F_3$–$^5I_8$, and $^5S_2$–$^5I_8$ fluorescence intensities which can be related to n_i by equation $I_i = h\nu_{io} W_{io} n_i$ [2] are described by the expressions

$$I_6(^5G_5) = \frac{h\nu_{60} W_{60} W_{32} U_{03} U_{26} N_0 \phi^2}{\tau_6^{-1}(C_3 + \tau_3^{-1})(C_2 + \tau_2^{-1})}, \quad (10)$$

$$I_5(^5F_3) = \frac{h\nu_{50} W_{50} W_{32} W_{21} U_{03} U_{15} N_0 \phi^2}{\tau_5^{-1}(C_3 + \tau_3^{-1})(C_2 + \tau_2^{-1})(C_1 + \tau_1^{-1})}, \quad (11)$$

$$I_4(^5S_2) = \frac{h\nu_{40} W_{40} W_{32} U_{03} N_0 \phi^2}{(C_4 + \tau_4^{-1})(C_3 + \tau_3^{-1})(C_2 + \tau_2^{-1})} \times \left[\frac{W_{21} W_{54} U_{15}}{\tau_5^{-1}(C_1 + \tau_1^{-1})} + \frac{W_{64} U_{26}}{\tau_6^{-1}}\right]. \quad (12)$$

One can notice from these expressions that the $^5G_5$–$^5I_8$, $^5F_3$–$^5I_8$, and $^5S_2$–$^5I_8$ fluorescence intensities have the characteristic square-law dependence on the incident pump flux at low excitation intensities. Fig. 7 shows the dependences of these fluorescence intensities on the absorbed pump power. The quadratic dependences expected from the Eqs. (10)–(12) fit the experimental data very well at lower pumping intensities, proving that the upconversion processes requires two photons. However, at higher pump powers, the fluorescence intensities depend upon the excitation intensity with lower slopes than two and these dependences are gradually reduced from quadratic to linear as shown in Fig. 7. This reduction is because the analysis stated above will only be applicable at the pump power sufficiently low that a depletion of the ground state population can be neglected, but this approximation will be invalid at higher pumping intensities. To understand the effects of excitation power that would be expected, we assumed that the levels 1 and 2 are metastable and

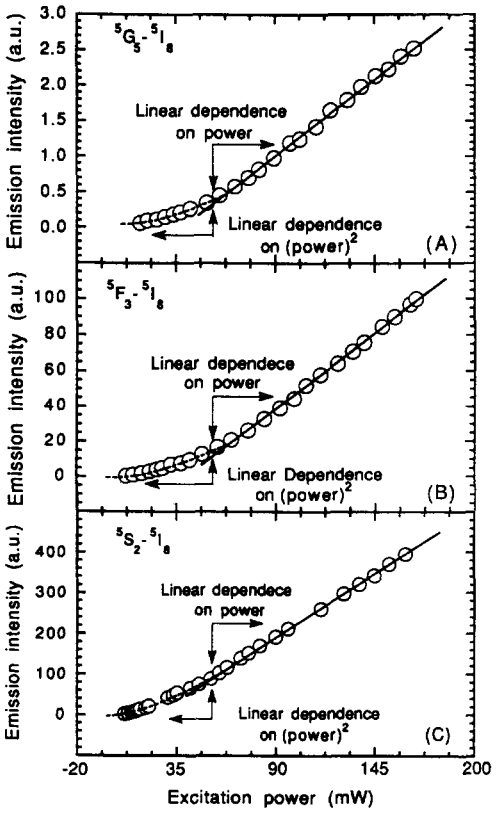

Fig. 7. Excitation-power dependences of the $^5G_5 - {}^5I_8$, $^5F_3$-^5I, and $^5S_2 - {}^5I_8$ fluorescence intensities for 0.5 mol% Ho^{3+} doped AZF glass excited at 647 nm.

their populations can build up to a larger value. Then the ground state population n_0 should be written as

$$n_0 = N_0 - n_1 - n_2 - n_3 - n_4 - n_5 - n_6 \cong N_0 - n_1 - n_2. \quad (13)$$

If we assume that the initial absorption of a photon can produce a significant population depletion of the ground state, the ground state population will be much smaller than the Ho^{3+} concentration. Then the Eq. (13) can be solved by combining the Eqs. (1)–(3), and the n_0 can be expressed as

$$n_0 = \frac{N_0}{1 + \dfrac{W_{32}U_{03}\phi}{(C_3+\tau_3^{-1})(C_2+\tau_2^{-1})}\left[1 + \dfrac{W_{21}}{(C_1+\tau_1^{-1})}\right]}. \quad (14)$$

The second and third terms in the denominator are responsible for the ground state depopulation and are appreciably larger than unity if depopulation is significant. The ground state population will therefore be inversely proportional to the incident pumping intensity as shown in the following equation:

$$n_0 \cong \frac{N_0(C_3+\tau_3^{-1})(C_2+\tau_2^{-1})(C_1+\tau_1^{-1})}{\phi U_{03}W_{32}\left[(C_1+\tau_1^{-1})+W_{21}\right]}. \quad (15)$$

Combining the expression for n_0 in Eq. (15) and the equation of $I_i = h\nu_{i0}W_{i0}n_i$ with Eqs. (7)–(9), the intensity of upconversion fluorescence, for example, from the $^5S_2$ level can be expressed as

$$I_4(^5S_2) \cong \frac{h\nu_{40}W_{40}(C_1+\tau_1^{-1})N_0\phi}{(C_4+\tau_4^{-1})\left[(C_1+\tau_1^{-1})+W_{21}\right]} \times\left[\frac{W_{21}W_{54}U_{15}}{\tau_5^{-1}(C_1+\tau_1^{-1})}+\frac{W_{64}U_{26}}{\tau_6^{-1}}\right]. \quad (16)$$

One can see that the fluorescence intensities corresponding to the $^5G_5$–$^5I_8$, $^5F_3$–$^5I_8$, and $^5S_2$–$^5I_8$ transitions will now be only directly proportional to the incident pumping intensity, ϕ. From Fig. 7 we can find that the linear dependences expected from the rate equation model fit the experimental data very well at higher pump powers. It well interprets why the output power was linearly dependent on pump power despite the fact that the green upconversion fluorescence requires two photons as reported by

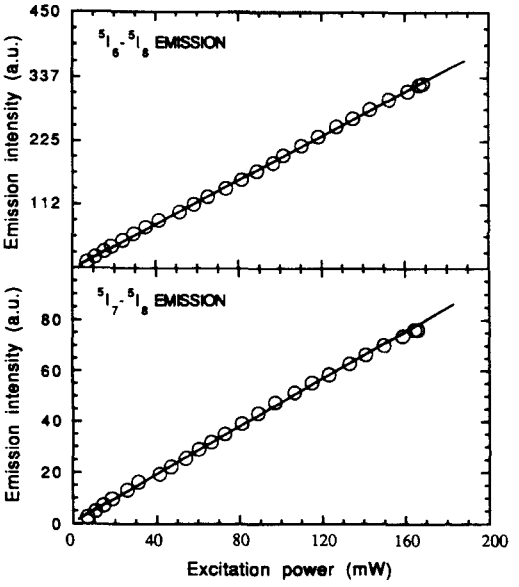

Fig. 8. Excitation-power dependences of the $^5I_6$–$^5I_8$ and $^5I_7$–$^5I_8$ fluorescence intensities for 0.5 mol% Ho^{3+} doped AZF glass excited at 647 nm.

Allain et al. [10]. Indeed, at higher pump powers, a saturation effect reduces the pump power dependences of the fluorescences. There are two possible processes that may cause the saturation effect. The first is the depletion of the ground state population by the optical pump, corresponding to the saturation of the $^5I_8$–$^5F_5$ transition. A second process results when the rate of depopulation of a intermediate level by upconversion exceeds the spontaneous and nonradiative emission rates from this level [13]. Since intensities of both the fluorescences originating from the intermediate levels of $^5I_6$ and $^5I_7$ have characteristic linear-law dependences on the incident pump power as shown in Fig. 8, the intermediate levels are considered to be not significantly depopulated by ESA. The saturation effect is therefore only attributed to the former mechanism, i.e., the initial absorption of a photon can produce a significant depletion of the ground state population which saturates at relatively high pump powers. Also, this population depletion of the ground state is observed to saturate at about 60 mW which below laser threshold pump power of 147 mW [14], indicating that the rate limiting step in the excitation process is the absorption of the second pump photon, by either

of the two parallel paths. It gives rise to a linear, rather than quadratic, dependence of output power on pump power.

4.2. Concentration dependence of the upconversion fluorescences

It is noteworthy that the effect of energy transfers among Ho^{3+} ions involving concentration quenching always appear in the system and this effect is to reduce the observed fluorescence intensity by an amount that depends on the ratio of the energy transfer rate C_i to the intrinsic depopulation rate W_{ij}. If the energy transfer rates can be negligible compared to the intrinsic decay rates, the fluorescence intensities will be directly proportional to the Ho^{3+} concentration and lifetimes of the emitting and intermediate levels as shown in Eqs. (10)–(12). However, from Fig. 4 it can be seen that the $^5G_5$–$^5I_8$ and $^5S_2$–$^5I_8$ fluorescence intensities do not increase monotonically with increasing the Ho^{3+} concentration except for the $^5F_3$–$^5I_8$ fluorescence. This behavior is undoubtedly ascribed to the energy transfers among Ho^{3+} ions in the system. In general, the energy transfer rates increase when the interactive ion concentration increases. If the energy transfer rates C_i become larger than the intrinsic decay rates W_{ij} for some levels, the concentration dependences can be lowered or eliminated depending upon the levels. The advantage of a long intermediate level lifetime is also lost if the energy transfer from that level is high. For instance, with increasing the concentration of Ho^{3+} in AZF glass system, the lifetime of the $^5I_6$ intermediate level from which a part of the excited Ho^{3+} ions can be re-excited to the $^5G_5$ emitting level by ESA rapidly decreases as shown in Fig. 9 due to the so-called 'concentration quenching', emphasizing significant depopulation of that level. It is therefore impossible that the upconversion fluorescence from the $^5G_5$ level required to be populated by ESA from the $^5I_6$ level increases monotonically with increasing the Ho^{3+} concentration. At lower concentrations, the effect of energy transfer from the $^5I_6$ intermediate level is sufficiently low that the upconversion fluorescence intensity increases regularly. At higher concentrations, however, the energy transfer rate becomes so large that the $^5I_6$ level is considerably depopulated to reduce the upconversion efficiency from this level to the $^5G_5$ level, and thereby making the $^5G_5$–$^5I_8$ fluorescence decreased after the maximum value taken place as shown in Fig. 4(a).

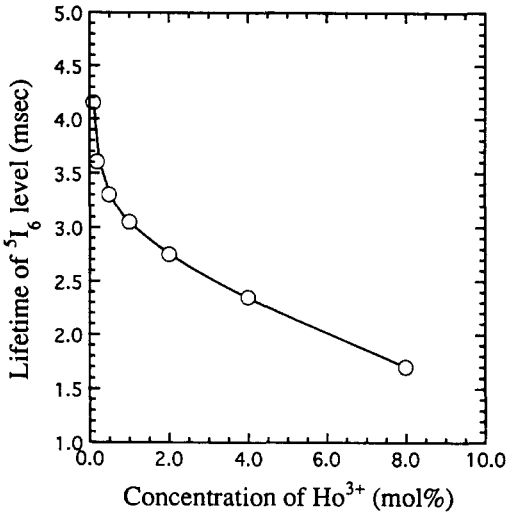

Fig. 9. Concentrational dependence of the $^5I_6$ lifetime of Ho^{3+} in AZF glass excited at 645 nm. Line is a guide to the eye.

Similarly, for understanding the concentration dependence of upconversion fluorescence from the $^5F_3$ level, the population of the corresponding intermediate level of $^5I_7$ must be estimated at first, since the energy transfer from the $^5F_3$ level as well as the $^5G_5$ level is inexistent in the system. The fluorescence and lifetime required to estimate the population of the $^5I_7$ level were measured and plotted in Fig. 10 as a function of the Ho^{3+} concentration for AZF glass. The fluorescence intensity and lifetime of this intermediate level increase monotonically with increasing the Ho^{3+} concentration due to the following possible cross relaxations of [14]

$^5F_5$–$^5I_6$ to $^5I_8$–$^5I_7$,

$^5S_2$–$^5I_4$ to $^5I_8$–$^5I_7$,

$^5S_2$–$^5I_7$ to $^5I_8$–$^5I_4$,

which can cause the $^5F_5$ and $^5S_2$ lifetimes to be decreased and the $^5I_7$ intermediate level to be populated. The $^5F_5$ and $^5I_7$ lifetimes, which have been illustrated in Figs. 5 and 11, rapidly decrease as the Ho^{3+} concentration increases, indicating that the energy transfers from the $^5F_5$ and $^5S_2$ to the $^5I_7$ are very sensitive to the Ho^{3+} concentration, i.e., these

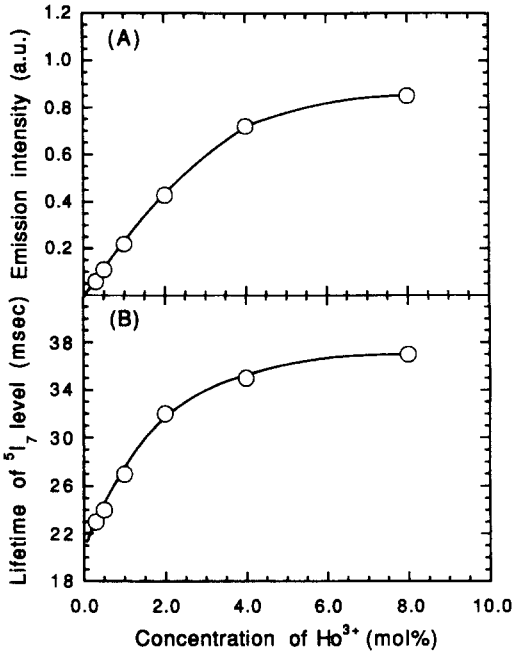

Fig. 10. Concentrational dependences of the $^5I_7-^5I_8$ fluorescence intensity and the $^5I_7$ lifetime of Ho^{3+} in AZF glass. Lines are a guide to the eye.

energy transfer rates can be enhanced by increasing the Ho^{3+} concentration. This is because the non-resonant energy transfer rate is, in general, inversely proportional to the intrinsic distance between the interactive ion pairs and this distance will be shorter if the Ho^{3+} concentration is high. Obviously, all of these energy transfers can cause the $^5I_7$ intermediate

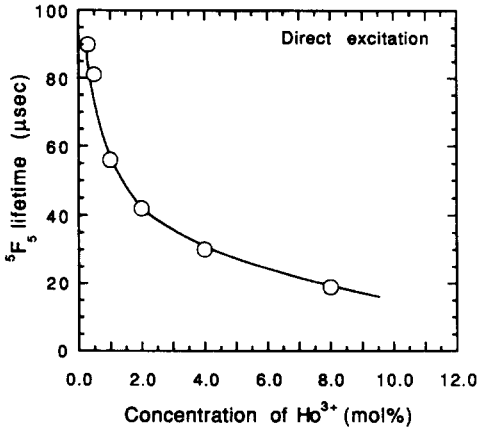

Fig. 11. Concentrational dependence of the $^5F_5$ lifetime of Ho^{3+} in AZF glass excited at 645 nm. Line is a guide to the eye.

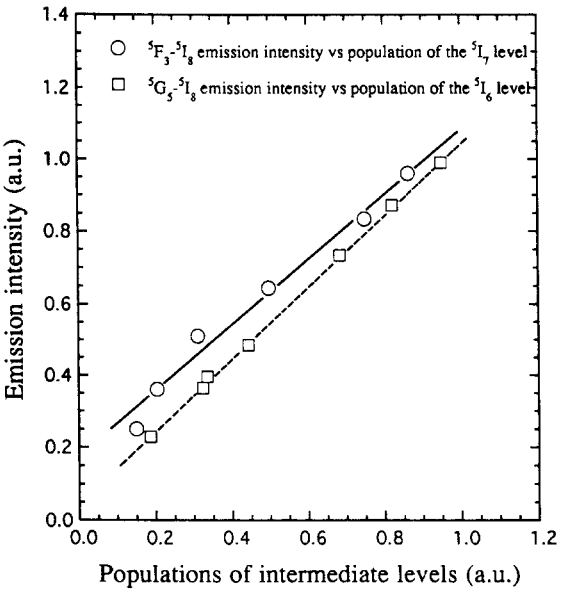

Fig. 12. Relationship between the $^5G_5-^5I_8$ and $^5F_3-^5I_8$ fluorescence intensities and the populations of the intermediate levels of $^5I_6$ and $^5I_7$. Lines are a guide to the eye.

level to be populated and thus gives rise to a high upconversion efficiency from this level to the $^5F_3$ level by absorbing a second photon. It is therefore concluded that a monotonical increase in the upconversion fluorescence from the $^5F_3$ level with increasing the Ho^{3+} concentration is due to an increase in population of the corresponding intermediate level.

In order to further understand the correlation between populations of the emitting level and the corresponding intermediate level, we plotted the intensities of upconversion fluorescences from the $^5G_5$ and $^5F_3$ levels in Fig. 12 versus relative populations of the corresponding intermediate levels of $^5I_6$ and $^5I_7$. All the upconversion fluorescence intensities have the characteristic linear-law dependences on the populations of the intermediate levels. It reveals that the blue upconversion fluorescences of the Ho^{3+} doped system is primarily determined by the populations of the corresponding intermediate levels of $^5I_6$ and $^5I_7$.

However, the $^5S_2$ emitting level is distinguishable from the $^5G_5$ and $^5F_3$ levels. This level is populated by de-excitations from the upper $^5F_3$ and $^5G_5$ levels but not by ESA directly from intermediate level. Since the multiphonon relaxation rates of the $^5G_5$ and $^5F_3$ levels are more than 10×10^5 and 4.5×10^5

s^{-1} which are far greater than their spontaneous emission rates of 2580 and 1665 s^{-1}, respectively, a great part of the excited ions in the $^5G_5$ and the $^5F_3$ levels are non-radiatively de-excited to the $^5F_3$ level and then to the $^5S_2$ level. This fact shows that the $^5S_2$ emitting level is mainly populated from the upper excited $^5F_3$ level by the multiphonon relaxation. If the energy transfer from the $^5S_2$ level is taken no account, the concentration dependence of the upconversion fluorescence from the $^5S_2$ level ought to have been agreement with that from the $^5F_3$ level. Comparing the results in Fig. 4, however, it can be seen that the concentration dependence of the $^5S_2$–$^5I_8$ fluorescence is distinguishable from that of the $^5F_3$–$^5I_8$ fluorescence. It indicates that the variation behavior of the upconversion fluorescence from the $^5S_2$ level against the Ho^{3+} concentration is only interpreted by the energy migrations between Ho^{3+} ion pairs through the $^5S_2$ level. The non-exponential decays of the $^5S_2$ level and the rapid decrease of the phenomenon (as shown in Fig. 5) reveal that the quick energy transfers of

$^5S_2$–$^5I_4$ to $^5I_8$–$^5I_7$

and

$^5S_2$–$^5I_7$ to $^5I_8$–$^5I_4$

occur in the system. When the $^5S_2$ level is populated, the closest interactive ion pairs rapidly undergo energy transfer initially and therefore their population becomes depleted early in the decay. The depletion continues radially outward from the donor ions as time progresses until the only pairs remaining are sufficiently separated the energy transfer does not occur. The decay has then resumed the intrinsic exponential decay. The energy transfers between Ho^{3+} ion pairs are so efficient at higher concentrations (as shown in Fig. 5) that the $^5S_2$ level is significantly depopulated and thus causes the upconversion fluorescence intensity to be lower.

5. Conclusion

The blue and green upconversion fluorescences originating from the $^5G_5$, $^5F_3$, and $^5S_2$ levels of Ho^{3+} were observed in several fluoride glasses under the 647 nm excitation. The relative intensities of these upconversion fluorescences for ZrF_4 (HfF_4) based glasses are more intense than those for AlF_3 based glasses due to their lower phonon energies. The upconversion and fluorescence efficiencies of Ho^{3+} doped fluoride system are primarily determined by the populations of the corresponding intermediate levels such as $^5I_6$ and $^5I_7$, and by the energy transfers from the emitting and intermediate levels. Rate equation modeling of the upconversion fluorescence of Ho^{3+} doped fluoride glass has been established and has been utilized to reveal the upconversion mechanism that the observed linear dependence on pump power is shown to arise primarily from the absorption of the second photon in the upconversion route. Using this model, the concentration dependences of the upconversion fluorescences can be well interpreted. The concentration dependences of the blue upconversion fluorescences $^5G_5$–$^5I_8$ and $^5F_3$–$^5I_8$ are strongly impacted by the energy transfers from the intermediate levels of $^5I_6$ and $^5I_7$, but the green upconversion fluorescence $^5S_2$–$^5I_8$ is mainly affected via the energy transfers from the emitting level of $^5S_2$.

References

[1] F.E. Auzel, Proc. IEEE 61 (1973) 758; Phys. Rev. B13 (1976) 2809.
[2] J.C. Wright, in: Topics in Applied Physics, Vol. 15, ed. F.K. Fong (Springer, Berlin, 1976) p. 239.
[3] A.A. Bergh and P.J. Dean, Light-Emitting Diodes (Clarendon, Oxford, 1976) p. 343.
[4] R.M. Macfarlane, F. Tong, A.J. Silversmith and W. Lenth, Appl. Phys. Lett. 52 (1988) 1300.
[5] S.A. Pollack, D.B. Chang and M. Birnbaum, Appl. Phys. Lett. 54 (1989) 869.
[6] J.Y. Allain, M. Monerie and H. Poignant, Electron. Lett. 26 (1990) 166.
[7] R.A. Mcfarlane, Appl. Phys. Lett. 54 (1989) 2301.
[8] R.G. Smart, D.C. Hanna, A.C. Tropper, S.T. Davey, S.F. Carter and D. Szebesta, Electron. Lett. 27 (1991) 1307.
[9] K. Hirao, S. Todoroki and N. Soga, J. Non-Cryst. Solids 143 (1992) 40.
[10] J.Y. Allain, M. Monerie and H. Poignant, Electron. Lett. 26 (1990) 261.
[11] F. Tong, W.P. Risk, R.M. Macfarlane and W. Lenth, Electron. Lett. 25 (189) 1389.
[12] K. Hirao, S. Kishimoto, K. Tanaka, S. Tanabe and N. Soga, J. Non-Cryst. Solids 139 (1992) 151.
[13] J.E. Geusic, F.W. Ostermayer, H.M. Marcos, J.P. van der Ziel and L.G. Van Uitert, J. Appl. Phys. 42 (1971) 1958.
[14] G.R. Atkins, M.G. Sceats and S.B. Poole, J. Non-Cryst. Solids 140 (1992) 123.